

Tumor Detection in Mammography Images using Discrete Wavelet Transform and Bayes Fusion Technique

Abdelkader Zitouni¹, Fatiha Benkouider¹, Fatima Chouireb¹ and Mourad Reggab¹

¹ University Amar Telidji, 37G Route de Ghardaia, Laghouat, 03000, Algeria

Abstract

This research presents supervised classification algorithm based on information fusion for detecting masses in mammography images. Discrete wavelet transform can preserve information regarding both high and low frequencies and offer great discriminatory power between areas with strong similarities. This motivates us to use this type of features to improve image segmentation. So, in the first stage, the suggested technique used this feature extraction approach on mammography images in order to obtain additional information. After that in the second stage, estimated feature vector of each pixel is sent to a neural network classifier for initial-labeling. Then, in the third stage of the suggested technique, Bayes fusion method is used to combine the scores, within a sliding window, obtained by the neural network for each pixel. The performance of the proposed segmentation algorithm was evaluated on mammography images from Mammography Image Analysis Society (MIAS) dataset. The achieved classification results by the proposed fusion system leads to higher classification precision in detecting masses on mammography images, which are one of breast cancer signs.

Keywords

Image segmentation, Masses Detection, Breast Cancer, Neural Network, Wavelets, Bayes fusion.

1. Introduction

One of the leading causes of death worldwide among women is breast cancer [1]. Studies on breast cancer have demonstrated that early detection of these abnormalities plays a very important factor in cancer treatment and allows better recovery for most patients [2].

Medical imaging is a robust and reliable diagnostic method for the breast related diseases and it can be produced from various equipment in the medical field, such as Ultrasound (USG), MRI, CT-Scan / CAT-Scan, and Mammography [3].

Mammography is the major screening tool which is carried out for detection of breast cancer at early stage, and several images processing techniques have been used for mammograms interpretation in order to assist radiologists while detecting or identifying eventual abnormalities [4-18]. [4] and [5] presented an automated classification of breast cancer lesions using neural networks and deep belief network; [6], [7], [8] used gray-level co-occurrence matrix for mammograms classification; [10], [11] proposed a mammogram classification scheme using 2d discrete wavelet and local binary pattern.

Generally, masses (space occupying lesions) and calcifications (tiny flecks of calcium, like grains of salt) are the two abnormalities present in the mammogram images. The pre-processing and feature extraction process is an important stage in identifying the presence of tumors. So, referring to the

RIF'23 : The 12th Seminary of Computer Science Research at Feminine, March 09, 2023, Constantine, Algeria

EMAIL: a.zitouni@lagh-univ.dz (A. Zitouni); fbenkouider@gmail.com (f. Benkouider); f.chouireb@lagh-univ.dz (F. Chouireb); m.reggab@lagh-univ.dz (M. reggab)



© 2023 Copyright for this paper by its authors.
Use permitted under Creative Commons License Attribution 4.0 International (CC BY 4.0).
CEUR Workshop Proceedings (CEUR-WS.org)

advantages and disadvantages of the methods and algorithms that have been developed by previous researchers, in this paper we attempt to use one type of feature extraction techniques with the purpose of detecting masses on mammography images. This feature is a structural feature obtained by using the wavelet transform coefficients. For the pre-processing process, which finds to improve image quality such as contrast enhancement to obtain a better image visualization [1], there are different types of filtering techniques. In this study the contrast of the mammogram images was regulated by histogram adjustment which improves the contrast of the output image by spreading out the intensity values.

So, in the first stage of our work, we have used the discrete wavelet transform as feature extraction strategy in order to get more information that enables the classifiers to discriminate between the different areas in the mammography image. In the second stage, an appropriate classification algorithm is applied using the set of extracted features obtained from the previous stage. The Backpropagation Artificial Neural Networks classifier is chosen among the most well-known classifiers, it was initiated in [19-20]. The estimated feature vector of each pixel is sent to the neural networks classifier for initial-labeling.

A sliding window, whose class is assigned to its central pixel, is used. However, this central pixel belongs to other window neighbors that may be classified into other classes. Consequently, in the third stage, in order to obtain a more precise segmentation result, a Bayes fusion method is used for each pixel to combine the scores results of several windows that contain this central pixel. The proposed segmentation algorithm performance was verified on mammography images from MIAS dataset [21]. The obtained results lead to higher classification precision in detecting masses which are one of breast cancer signs.

The rest of this manuscript is divided in three sections. The first one describes the background theory of several techniques used in this paper. Then, section 2 is dedicated to give in details the suggested segmentation process and the reached performance of the proposed fusion technique. Finally, in section 3, we conclude and recommend possibilities for future work.

2. Feature Extraction Algorithm and Fusion Theory

2.1 The wavelet analysis

Since the work of Grossman and Morlet [22], the wavelets transform has appeared as a powerful tool to solve problems in different application. The wavelets transform decomposes the input signal into a series of wavelet functions $\Psi_{a,b}(t)$ derived from a mother function $\Psi(t)$ given by dilatation (factor a) and translation (factor b) operations. Figure1 illustrates some examples of wavelets that are generally used in image processing [23].

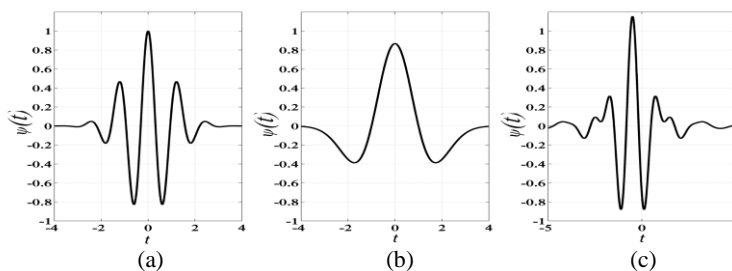


Figure 1: Examples of wavelets.

(a) Morlet Wavelet, (b) Mexican hat Wavelet, (c) Meyer Wavelet

Wavelet analysis transforms a finite energy signal in the spatial domain into another finite energy signal in the spatio-frequency domain. The components $C_{a,b}$ of this novel signal, which are described in equation (1), are called wavelet coefficients. In an image, these coefficients offer information on the local variation of the grey levels around a given pixel. The more significant is this variation, the higher they are [24].

$$C_{a,b} = \int_{-\infty}^{+\infty} x(t)\Psi_{a,b}(t)dt, \quad (1)$$

where

$$\Psi_{a,b}(t) = \frac{1}{\sqrt{a}}\psi\left(\frac{t-b}{a}\right) \quad \text{with } a \neq 0 \quad (2)$$

The most important advantage of wavelets as compared to other frequency methods, as Fourier transform, is that it offers both frequency and spatial locality [25]. In 1989, Mallat [26] suggested a multi-resolution decomposition algorithm based on wavelets transform. The algorithm decomposes an input image into a set of detail images and an approximation image using a filter bank comprising a high pass filter (HP) and a low pass filter (LP). At each decomposition level the size of the transformed images is reduced by a factor of two [24]. The discrete wavelet transform of a 2-D image can be obtained by performing the filtering consecutively along horizontal and vertical directions (separable filter bank) [27]. Four images are then created at each level. Figure 2 shows an example of decomposition of the image on one level.



Figure 2: Use of 1-stage discrete wavelet transform (DWT)

In Figure 2, the DWT decomposes the image into 4 orthogonal sub-band: low-low (LL), high low (HL), low high (LH), and high-high (HH) consisting of approximation, horizontal, vertical, and diagonal information. The approximations image is the smoothed version of the original image and it contains global information that is similar to the original image with the number of rows and the number of columns being half of the original image. Horizontal, vertical, and diagonal contain the detail and represent the fluctuations of the pixel intensity in horizontal, vertical, and diagonal directions and they have low-intensity areas, whereas areas with high intensity are only found on the edges of the image object.

The values of transformed coefficients in detail and approximation images (sub-band images) represent the necessary features that capture useful discrimination information for masses segmentation [28].

1. Wavelet's Choice: In our research, we have used a second order biorthogonal spline wavelet. This wavelet is used for masses analysis due to its excellent location in the frequency and spatial domains and its sensitivity to local singularity and correlation of the image [24].

2. Indices' Calculation: One of the most used indices for characterizing the masses in the spatio-frequency plane is the measurement of energy. Because the transformed images have different frequencies, scales and orientations, the energy index is a local measure of the wavelet coefficient distribution according to the scale, the orientation and the frequency. It has been used successfully for segmentation and classification of masses [24].

The expression of energy is given by [24]:

$$E = \frac{1}{N} \sum_R C(i,j)^2 \quad (3)$$

The second index used in conjunction with energy is the measurement of the local mean of the wavelet coefficients given by [24]:

$$M = \frac{1}{N} \sum_R |C(i,j)|, \quad (4)$$

where N denotes the number of pixels, designated by the indices (i,j) , and enclosed in the area R .

The calculation of these indices was done on a sliding window W . The local mean and the energy on the sliding window are calculated from the resultant sub-band images. So the feature vector of each window is made of eight parameters $V = [E_{LL}, E_{LH}, E_{HL}, E_{HH}, M_{LL}, M_{LH}, M_{HL}, M_{HH}]$, as seen in Figure 3.

Several tests were carried out on a series of window sizes going from 5×5 to 25×25 . The highest good classification rate was reached for a window of dimension 11×11 . The produced features vector of each window is used as an input to the neural network classifier for a primary labeling, and the score for the window delivered by the neural network is assigned to its mid pixel.

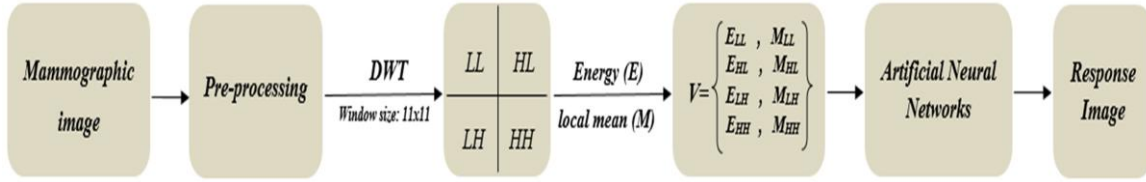


Figure 3: Wavelet features extraction stage

2.2 Theory of Bayes' Fusion

One of the first techniques used to combine images with decision-making was the Bayes fusion. This model was chosen by several authors because it has a very well-defined context with known mathematical properties [29].

Consider H_1, H_2, \dots, H_N to be a collection of mutually exclusive hypotheses. They satisfy the following conditions:

$$\begin{cases} \forall i, j, H_i \cap H_j = \emptyset, & i \neq j, \\ \cup_{i=1}^N H_i = E, \end{cases} \quad (5)$$

where E represents the hypothesis' space (that is to say, the set of fused image classes). The hypotheses are mutually exclusive and form a partition of E .

Consider m_1 and m_2 to be two characteristic primitives from two different images, representing the same object, or the same hypothesis H_i , the Bayesian theory computes the likelihood of getting the hypothesis H_i from the two measures m_1 and m_2 through Bayes rule [30]:

$$P(H_i/m_1, m_2) = \frac{P(H_i) \cdot P(m_1, m_2/H_i)}{\sum_{j=1}^N P(H_j) \cdot P(m_1, m_2/H_j)}, \quad (6)$$

where $P(m_1, m_2/H_i)$ represents the joint probability of having both measures (m_1, m_2) once the hypothesis H_i is realized, and $P(H_i)$ is the prior probability of the hypothesis H_i , which shows the possibility of occurrences of the hypothesis H_i in the general case [30].

If m_1 and m_2 are two independent random variables, the conditional probability $P(m_1, m_2/H_i)$, also called the likelihood function, becomes a separable function of the two variables m_1 and m_2 .

$$P(m_1, m_2/H_i) = P(m_1/H_i) \cdot P(m_2/H_i) \quad (7)$$

Hence equation (6) takes the following form:

$$P(H_i/m_1, m_2) = \frac{P(H_i) \cdot P(m_1/H_i) \cdot P(m_2/H_i)}{\sum_{j=1}^N P(H_j) \cdot P(m_1/H_j) \cdot P(m_2/H_j)} \quad (8)$$

Consequently, in order to determine the posterior probabilities $P(H_i/m_1, m_2)$, we first need to compute the prior probabilities $P(H_i)$ for all hypotheses H_i , i going from 1 to N , and the likelihood functions $P(m_j/H_i)$ for each image primitive m_j and for each hypothesis. To model the likelihood functions, we work under the Gaussian hypothesis [30]:

$$P(m_j/H_i) = \frac{1}{\sigma_i \sqrt{2\pi}} \exp\left(-\frac{(m_j - \bar{H}_i)^2}{2\sigma_i^2}\right), \quad (9)$$

where \bar{H}_i denotes the mean and σ_i is the standard deviation of the Gaussian expression.

When the combination of the probabilities realized by equation (8), we have to select a decision's criterion to decide which hypothesis H_i is supposed to be chosen according to all posterior probabilities. Many criteria are suggested in the literature: The maximum of posterior probability is the most commonly used criterion, which selects the hypothesis H_i having the highest probability $P(H_i/m_1, m_2)$ [31].

3. The Proposed Segmentation Algorithm

Data obtained from the mammographic images is often, noisy, incomplete, inconsistent, and have low contrast. Therefore, pre-processing is needed in the medical image processing to improve image quality, remove unwanted noise, preserves the edges within an image, and make the feature extraction phase more reliable [1].

There are different types of filtering techniques in the pre-processing. So, in the first step of our work, the contrast of the mammogram images was regulated by histogram adjustment which increases and improves the contrast of the output image by spreading out the intensity values.

After that in the second step, the proposed segmentation method uses Wavelets transform as feature extraction strategy on mammography images in order to get more information in this data set. The parameters of the feature set were selected as mentioned in the previous sections. After a proper features' extraction, each estimated feature vector of each pixel is sent to the neural networks classifier for primary labeling. The MLP neural networks classifier is chosen among the most well-known classifiers, it was initiated in [19], [20]. For the choice of the hidden layers' number and the number of neurons in each layer, we choose the rule proposed by [34] since there is no general rule other than rules of thumb as proposed in [35], [36]. The size of the hidden layer is 75% of the input layer.

For the transfer functions, we retain the most used in the literature, namely the logistic function and the hyperbolic tangent function. The gradient backpropagation algorithm is used for the training of neural networks.

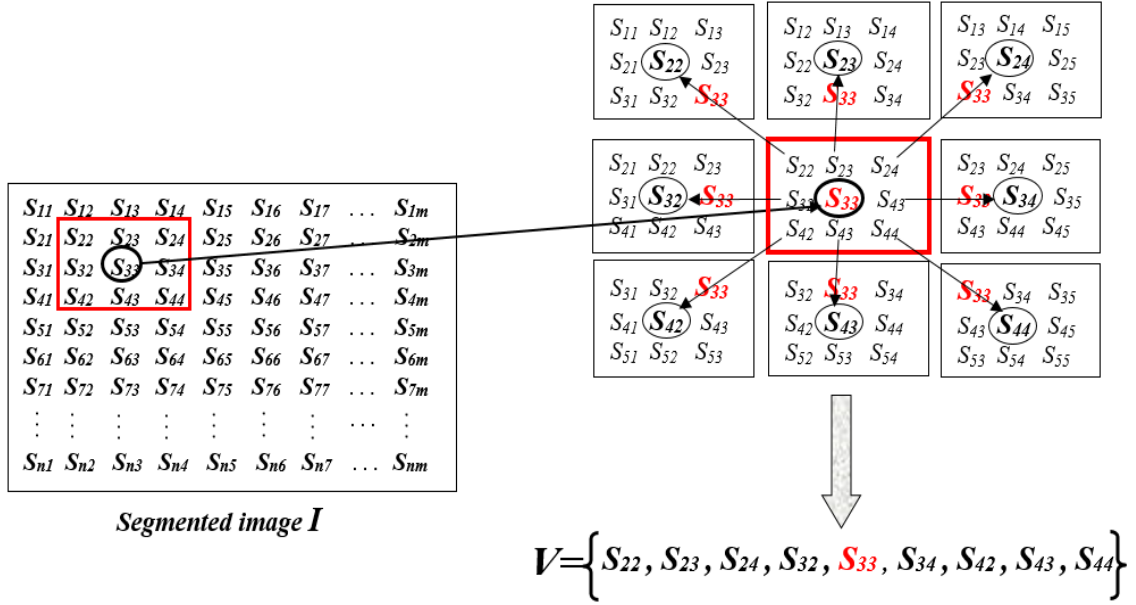


Figure 4. Composition of the fusion vector

Using a sliding window, the class for this window is assigned to its central pixel. However, this central pixel belongs to other window neighbors that may be classified into other classes. Consequently, in order to achieve a more precise segmentation result, for each pixel a Bayes fusion method is used to combine the scores results of several windows that contain this central pixel:

Consider I to be the segmented image comprising the scores S_{ij} of each pixel (the output of the neural networks classifier):

$$I = S_{ij} \text{ with } i=1 \dots n, j=1 \dots m,$$

where n and m represent the sizes of the mammography image.

We perused the images by using a sliding window of size $M \times M$, so that every pixel is surrounded by $M^2 - 1$ pixels. Each central pixel $P_{ij,l}$ of window W_l with score $S_{ij,l}$ belongs to the $M^2 - 1$ window in the surrounding windows before the classification process. However, each central pixel $P_{ij,z}$ of the window z , with $z = 1 \dots M^2 - 1$ produced different scores $S_{ij,z}$.

For example, in the case of pixel $P_{3,3}$ with score $S_{3,3}$ and $M = 3$, the central pixel is surrounded by eight pixels, that are the center of the eight windows which pixel $P_{3,3}$ belonged to, (see Figure 4).

From the above example, we joined the scores produced by the current block and its eight neighboring ones for the wavelet features: $\{S_{33}, S_{32}, S_{34}, S_{23}, S_{24}, S_{22}, S_{42}, S_{44}, S_{43}, S_{33}, S_{32}, S_{34}, S_{23}, S_{24}, S_{22}, S_{42}, S_{44}, S_{43}\}$ (see Figure 5). In this work, a sliding window of size 9×9 is used, so the central pixel is surrounded by 80 pixels, that are the center of the 80 windows which pixel $P_{5,5}$ belonged to.

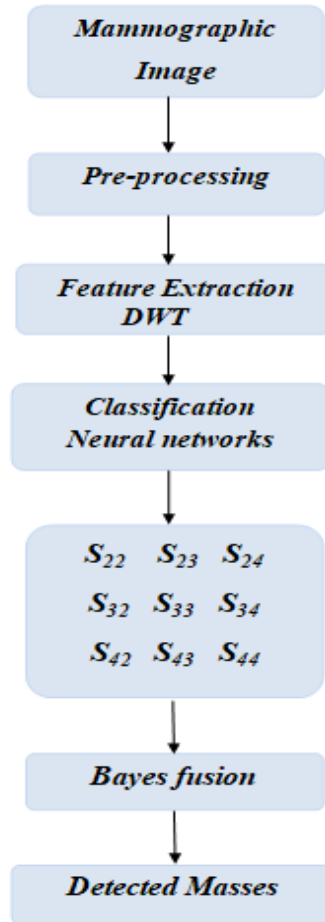


Figure 5. Classification stages block diagram

The essential fusion algorithm steps are summarized as follows:

Step1: Pre-processing of the mammography image.

Step2: Feature extraction via DWT.

Step3: Neuronal classification of the estimated feature vector. We obtain:

Step4:	<p><i>Scores1</i>: for DWT.</p> <p>while the recognition rate is changed</p> <p>do</p> <p> for each pixel do</p> <p> Bayesian fusion of Score1 and the neighboring scores.</p> <p> end</p> <p>end</p> <p>Calculate the recognition rate.</p> <p>End</p>
---------------	---

The performance of the proposed algorithm for segmenting mammography images is assessed using many images from the MIAS (Mammographic Image Analysis Society) database [21] containing 322 mammograms sized 1024 x 1024 pixels. The images are arranged in pairs: those with even-numbers correspond to left MLO (medio-lateral oblique Mammograms) and those with odd-numbers are right MLO.

For the learning phase, we have used image mdb028 of the MIAS database, and to test our algorithm we have taken randomly the following MIAS images:

mdb025 and mdb132, for Well-defined/circumscribed masses (CIRC) [32].

mdb184, for Spiculated masses (SPIC) [32].

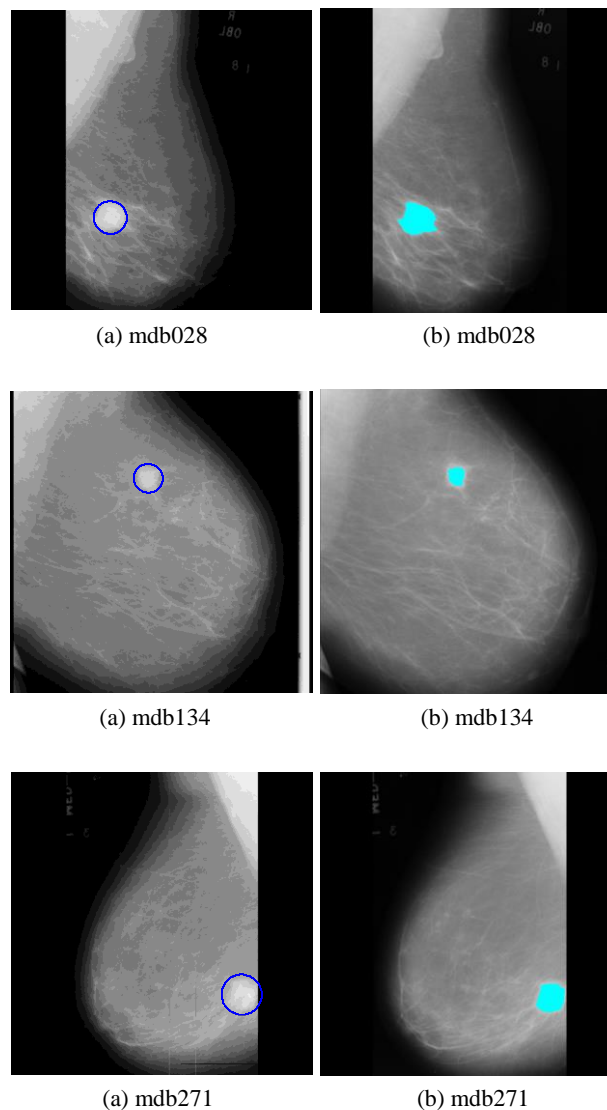
mdb134, mdb271 and mdb274, for Other, ill-defined masses (MISC) [32].

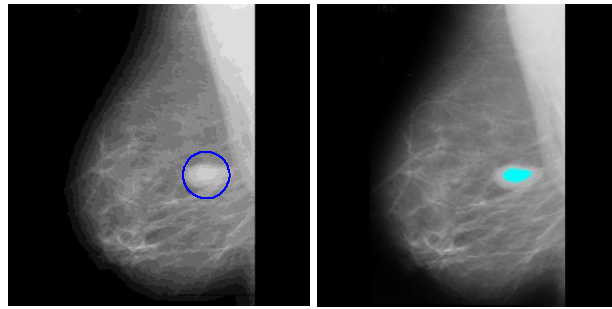
mdb136 and mdb310, for Normal breast (NORM) [32].

Figure 6 illustrates the obtained results (detected masses are displayed in cyan color) compared to expert decision (masses centers coordinates and radiuses shown in blue color). Table 1 demonstrates the Jaccard index that was achieved by utilizing this fusion algorithm.

So, as shown in figure 6 and table 1, the results obtained on these taken images from MIAS database are promising and they show the effectiveness of our fusion algorithm for the masses segmentation on mammography images.

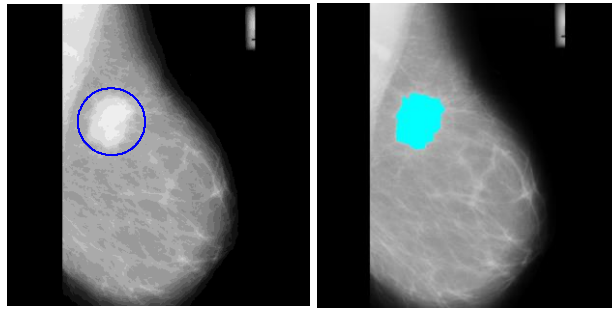
We can see clearly that our algorithm gives a good result whatever the kind of class of abnormality present, CIRC, SPIC, ... etc. And also, we don't have any false detection in the cases of normal breast. So, the proposed method has the potential to identify the presence of any masses in the mammogram image.





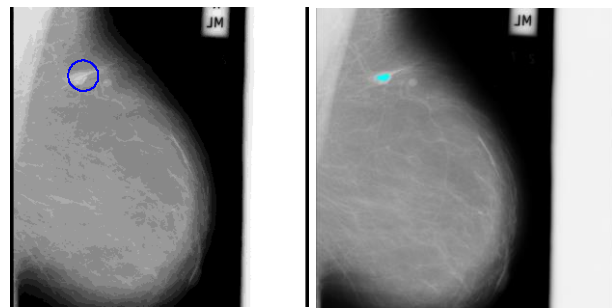
(a) mdb025

(b) mdb025



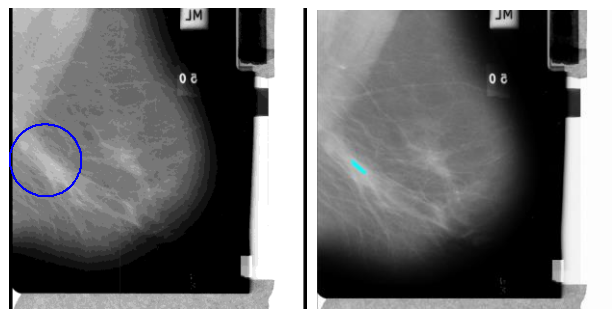
(a) mdb184

(b) mdb184



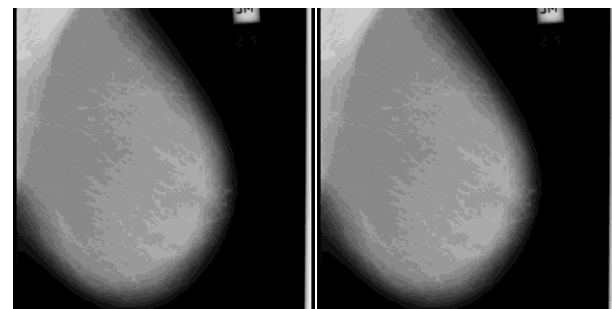
(a) mdb132

(b) mdb132



(a) mdb274

(b) mdb274



(a) mdb136

(b) mdb136

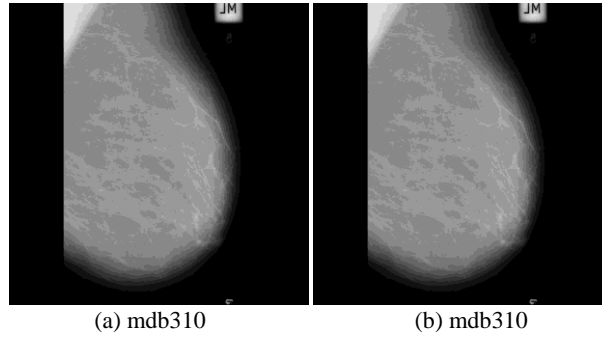


Figure 6: Experimental results on MIAS database: The first column (images a) contains the original mammograms with expert masse location. The second column (images b) represents the classification results using our approach.

Figure 7 illustrates a comparison of our proposed approach, on MIAS images mdb184 and mdb028, with another unsupervised techniques proposed by Kanta Maitra et al [33], based on Divide and conquer algorithm, and Boulehmi Hela et al [2], based on Generalized Gaussian Density.

As seen in figure 7, the proposed approach has the advantage of being simple and precise; we have exactly detected the shape of the present masses.

Table 1

Jaccard index of the fusion algorithm

Image	jaccard index (%)
mdb028	99.87
mdb134	99.77
mdb271	99.86
mdb025	99.41
mdb184	99.74
mdb132	99.83
mdb274	99.48
mdb136	100
mdb310	100

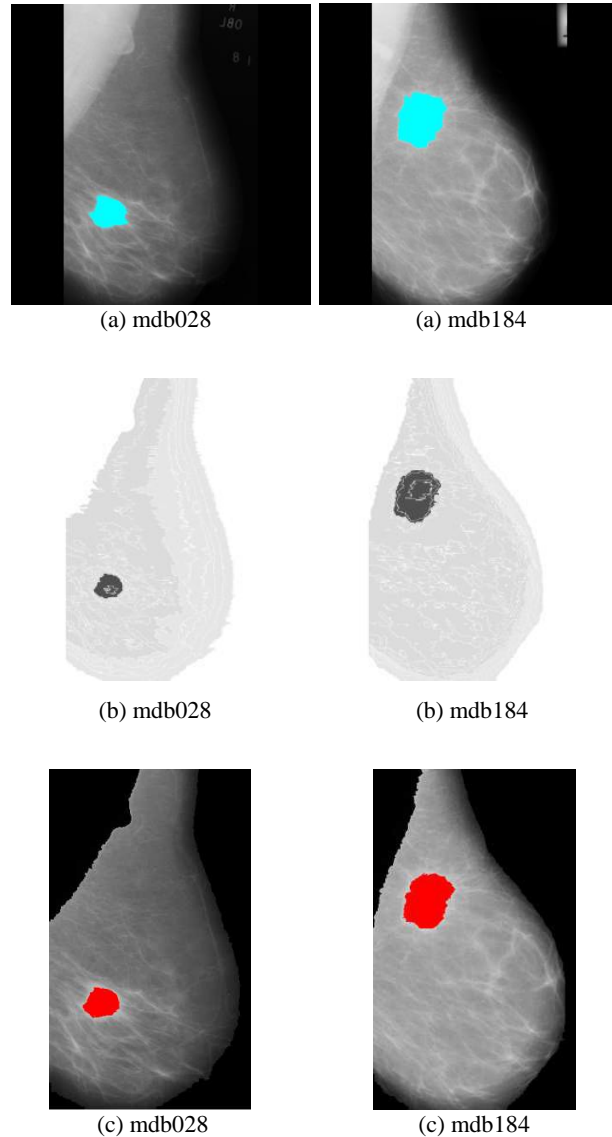


Figure 7: Comparison between results from:
 (a) Our approach, (b) [33], (c) [2].

The outcomes of our contribution demonstrate that it is possible to reach excellent fusion performance by neatly selecting the best fusion method. We also note that by our fusion method, the segmentation results of the mammography images are much improved as compared to other works.

4. Conclusion

In this article, we have presented and discussed a new approach for the segmentation of mammography images based totally on information fusion. We started by extracting the features using the wavelet transform. After that, the estimated vector of features for every pixel was sent to the neural network classifier for primary labeling. Next, a new fusion model for improving decision-making is used, it consists of combining the scores of each pixel within a sliding window. The proposed fusion algorithm was tested on mammography images from MIAS dataset.

This research has shown that this method is very effective for the automatic detection of abnormalities in digital mammogram.

As perspective we will complete the masses detection system by classifying abnormal mammographic images into benign and malignant.

5. References

- [1] M. Wisudawati Lulu, M. Sarifuddin, P. Wibowo Eri, A. Abdullah Arman, Feature Extraction Optimization with Combination 2D-Discrete Wavelet Transform and Gray Level Co-Occurrence Matrix for Classifying Normal and Abnormal Breast Tumors, *Modern Applied Science* 14 (15): 5 (2020).
- [2] H. Boulehmi, H. Mahersia, K. Hamrouni, Unsupervised Masses Segmentation Technique Using Generalized Gaussian Density, *International Journal of Image Processing and Graphics (IJIPG)*, 1, (2) (2013).
- [3] B. U. Fahnun, A. B. Mutiara, E. P. Wibowo, J. Arlan, A. Latief, Filtering techniques for noise reduction in liver ultrasound images, Phd thesis, Program Doktor Teknologi Informasi Universitas Gunadarma, (2018), 261–266. URL: <https://doi.org/10.1109/EIConCIT.2018.8878547>
- [4] M. M. Abdelsamea, M. H. Mohamed, M. Bamatraf, Automated classification of malignant and benign breast cancer lesions using neural networks on digitized mammograms, *Cancer Informatics*, 18, (2019), 1–3. Sage Journal. URL: <https://doi.org/10.1177/1176935119857570PMid:31244522 PMCID:PMC6580711>
- [5] D. Lestari, S. Madenda, J. Massich, A Segmentation Algorithm for Breast Lesion Based on Active Contour Model and Morphological Operations, *Advanced Science, Engineering and Medicine*, 7, 920-924. 10.1166/ase. (2015).1786. URL: <https://doi.org/10.1166/ase.2015.1786>
- [6] M. A. Al-antari, M. A. Al-masni, SU. Park et al, An Automatic Computer-Aided Diagnosis System for Breast Cancer in Digital Mammograms via Deep Belief Network, *J. Med. Biol. Eng.* 38, (2018), 443–456. URL: <https://doi.org/10.1007/s40846-017-0321-6>
- [7] M. Pratiwi, Alexander, J. Harefa, S. Nanda, Mammograms classification using gray-level co-occurrence matrix and radial basis function neural network, (2015). URL: <https://doi.org/10.1016/j.procs.2015.07.340>
- [8] R. Biswas, A. Nath, S. Roy, Mammogram classification using gray-level co-occurrence matrix for diagnosis of breast cancer, (2016), 161– 166. URL: <https://doi.org/10.1109/ICMETE.2016.85>
- [9] S. Ergin, I. Esener, T. Yuksel, A genuine glcm based feature extraction for breast tissue classification on mammograms, *International Journal of Intelligent Systems and Applications in Engineering*, (2016), 124– 124. URL: <https://doi.org/10.18201/ijisae.269453>
- [10] K. Ucar, H. E. Kocer, Breast cancer classification with wavelet neural network, *International Artificial Intelligence and Data Processing Symposium (IDAP)*, (2017), 1–5. URL: <https://doi.org/10.1109/IDAP.2017.8090347>
- [11] A. J. Putra, Mammogram classification scheme using 2d discrete wavelet and local binary pattern for detection of breast cancer, *Journal of Physics: Conference Series*, (2018). URL: <https://doi.org/10.1088/1742-6596/1008/1/012004>
- [12] M. Pawar, S. Talbar, Local entropy maximization-based image fusion for contrast enhancement of mammogram, *Journal of King Saud University Computer and Information Sciences*, (2018). URL: <https://doi.org/10.1016/j.jksuci.2018.02.008>
- [13] M. Pawar, S. Talbar, A. Dudhane, Local binary patterns descriptor based on sparse curvelet coefficients for false-positive reduction in mammograms, *Journal of healthcare engineering*, (2018). URL: <https://doi.org/10.1155/2018/5940436PMid:30356422 PMCID:PMC6178513>
- [14] Y. Shachor, H. Greenspan, J. Goldberger, A mixture of views network with applications to the classification of breast microcalcifications, *Computer Vision and Pattern Recognition*, (2018).
- [15] A. J. Bekker, M. Shalhon, H. Greenspan, J. Goldberger, Multi-view probabilistic classification of breast microcalcifications, in: *Proceedings of the IEEE Transactions on Medical Imaging*, 2016.
- [16] N. Dhungel, G. Carneiro, A. P. Bradley, Fully automated classification of mammograms using deep residual neural networks, in: *Proceedings of the 14th International Symposium on Biomedical Imaging (ISBI 2017)*, IEEE, 2017.
- [17] Y. Li, H. Chen, L. Cao, J. Ma, A survey of computer-aided detection of breast cancer with mammography, *J. Health Med. Inform.* 7 (4) (2016).

- [18] K. J. Geras, S. Wolfson, N. W. Y. Shen, S.G. Kim, E. Kim, L. Heacock, U. Parikh, L. Moy, K. Cho, High-resolution breast cancer screening with multi-view deep convolutional neural networks, in: Proceedings of the Computer Vision and Pattern Recognition, 2017.
- [19] J. Héroult, Ch. Jutten, Réseaux neuronaux et traitement du signal, Hermès, Paris, 1994.
- [20] J. F. Jodouin, Les réseaux de neurones. Principes et définitions, Hermès, Paris, 1994.
- [21] J. Suckling, J. Parker, D. Dance, S. Astley, I. Hutt, C. Boggis, I. Ricketts et al, Mammographic Image Analysis Society (MIAS) database v1.21 [Dataset], 2015. URL: <https://www.repository.cam.ac.uk/handle/1810/250394>
- [22] A. Grossman, J. Morlet, Decomposition of Hardy Functions into Square Integrable Wavelets of Constant Shape, SIAM Journal on Mathematical Analysis, 15, (4), 1984, pp. 723-736.
- [23] M. H. Sahbani, K. Hamrouni, Segmentation d'images texturées par transformée en ondelettes et classification C-moyenne floue, Proc. 3rd Int. Conf. Sciences of Electronic, Technologies of Information and Telecommunications, Tunisia, March 27-31, 2005.
- [24] T. Iftene, A. Safia, Comparaison Entre La Matrice De Cooccurrence Et La Transformation En Ondelettes Pour La Classification Texturale Des Images Hrv (Xs) De Spot, Télé-détection, 4, (1), (2004), pp. 39-49.
- [25] Ch. Anibou, M. N. Saidi, D. Aboutajdine, Classification of Textured Images Based on Discrete Wavelet Transform and Information Fusion, J. Inf. Process. Syst, 11, (3), (2015), pp. 421-437.
- [26] S. Mallat, A theory of multiresolution signal decomposition: the wavelet representation, IEEE Trans. Pattern Analysis and Machine Intelligence, 11, (7), (1989), pp. 674-693.
- [27] P. Scheunders, S. Livens, G. Van de Wouwer et al, Wavelet-based Texture Analysis, Int. J. Computer Science and Information Management, (1997).
- [28] S. Arivazhagan, L. Ganesan, Texture segmentation using wavelet transform, Pattern Recognition Letters, 24, (16), (2003), pp. 3197-3203.
- [29] A. Zitouni, F. Benkouider, F. Chouireb, M. Belkheiri, Classification of Textured Images Based on New Information Fusion Methods, IET Image Processing, vol.13, issue 9, (2019), pp. 1540 - 1549.
- [30] A. Dromigny-Badin, Fusion d'images par la théorie de l'évidence en vue d'applications médicales et industrielles, PhD. Dissertation, Institut National des Sciences Appliquées de Lyon, 1998.
- [31] A. Zitouni, Image Processing Methodology and Textures Analysis for their Segmentation, PhD. Dissertation, University Amar Telidji of Laghouat, Algeria, 2020.
- [32] The mini-MIAS database of mammograms. URL: <http://peipa.essex.ac.uk/info/mias.html>. Accessed 20 Dec 2020.
- [33] I. Kanta, S. Maitra, S. Nag, K. Bandyopadhyay, Detection of Abnormal Masses using Divide and Conquer Algorithm in Digital Mammogram, Int. J. Emerg. Sci., 1(4), (2011), 767-786.
- [34] B. Wierenga, J. Kluytmans, Neural nets versus marketing models in time series analysis: a simulation studies, in: Proceedings of the 23 annual conference "European marketing association", Maastricht, 1994, pp. 1139-1153.
- [35] V. Venugopal, W. Baets, Neural networks and statistical techniques in marketing research: A conceptual comparison, Marketing Intelligence and Planning, vol. 12, no. 7, (1994), pp. 30-38.
- [36] D. Shepard, The new direct marketing, Chapter Business one Irwin Homewood IL, Journal of Direct Marketing, vol. 6, (1992), pp. 52-53.